

**RERTR 2016 – 37<sup>TH</sup> INTERNATIONAL MEETING ON  
REDUCED ENRICHMENT FOR RESEARCH AND TEST REACTORS**

**OCTOBER 23-27, 2016  
RADISSON BLU ASTRID HOTEL  
ANTWERP, BELGIUM**

**2-D Fuel Meat Temperature Assessment of Full-Size Dispersion  
Fuel Plates**

Bei Ye, Aurelien Bergeron, Hannu Wallin, Gerard Hofman, Yeon Soo Kim  
Argonne National Laboratory, 9700 S Cass Ave., Lemont, IL 60439 – USA

Ann Leenaers, Vadim Kuzminov, Sven Van den Berghe  
SCK·CEN, Boeretang 200, B-2400 Mol - Belgium

**Abstract**

A 2-D FORTRAN framework was developed in order to improve the capability of the ANL-developed dispersion fuel performance code DART in simulating full-size fuel plates; 5 selected full-size U-7Mo/Al dispersion fuel plates irradiated in the BR2 reactor were simulated with the 2D framework. The calculations evaluated time-dependent fuel temperatures throughout a plate in both longitudinal and lateral directions, while updating fuel meat thermal conductivity at each time step. Additionally, profiles of plate thickness increase, fuel particle swelling, and constituent volume fractions as a function of fission density were generated. The calculated microstructural information at the end of the irradiations is in good agreement with the experimental data.

**1. Introduction**

Irradiation-induced interdiffusion between U-Mo particles and Al matrix is one of the phenomena suspected to limit overall fuel performance [1]. A thin coating layer (ZrN or Si) was applied on U-Mo particle surface as a diffusion barrier in the SCK·CEN SELENIUM test [2],[3]. Destructive examinations of the irradiated plates show that a small but significant amount of UMo-Al interdiffusion layer (IL) formed in high burnup region ( $> 4 - 4.5 \times 10^{21}$  fissions/cm<sup>3</sup>-UMo), but the IL formation is negligible at low burnup [4]. Hypotheses have been put forward to explain the IL formation behavior of coated particles. One possible explanation is that substantial IL growth occurs only in regions where the coating is damaged (bare contact between UMo and Al) and the temperature and fission rate are above a threshold value, resembling what was observed in chemical ion mixing experiments [5]. In order to verify the hypothesis, it is important to reasonably estimate fuel temperature distributions in the fuel plates during irradiation. However, it is impossible to measure fuel temperature during irradiation. Using a computation code implemented with adequate models therefore becomes the only plausible approach to evaluate the in-pile thermal performance of a fuel plate.

The ANL (Argonne National Laboratory)-developed dispersion fuel performance code - DART (Dispersion Analysis Research Tool) has been heavily used for fuel behavior modeling since its development in 1995 [6]. The code has been recently updated [7][8], and the validation results demonstrate that DART can reasonably reproduce U-Mo fuel in-pile test data [8][9]. However, the nodalization scheme in DART that only one node at a time for thermal solution along the axial direction makes it impossible to calculate full-size fuel plate temperature distribution and swelling behavior within reasonable computation time. In order to eliminate the inherent limitation of DART, a modernized FORTRAN 2-D framework was developed. It has a 2-D thermal solution and approximate models for the materials properties evolution implemented in the code, for example fuel meat thermal conductivity evolution, and will allow dual options for fuel swelling calculation (theory-based model or empirical correlation) in order to meet the different needs for fuel development and reactor analysis respectively.

In this paper, the fuel meat temperature profiles of 5 full-size U-7Mo/Al dispersion fuel plates irradiated in the Belgium BR2 reactor were calculated with DART-2D, including the fuel plates from SELENIUM, E-FUTURE, and SELENIUM-1a tests. The calculated fuel meat swelling and constituent volume fractions were compared to experimental observations. Details on the calculation scheme of DART-2D are also described.

## **2. Model description of the DART-2D framework**

In order to simulate fuel thermal performance, adequate mathematical models were brought together with a self-consistent approach in DART-2D. The program calculates temperature distribution, thermal conductivity, IL thickness, swelling, and fuel meat constituent volume fractions for a fuel plate during its operation – following its power history. A flow chart showing the order of the calculations in each time step is given in Fig. 1. The program requires certain inputs to perform the calculations, such as fuel plate and meat dimensions, coolant flow conditions, and power history. The code simulates one full-size plate at a time. Fig. 2(a) shows an example of the meshing scheme of a fuel plate in DART-2D. A symmetric configuration about the fuel meat center line is assumed. The color gradient is used to represent the temperature gradient (cold to hot, i.e. blue -> red). It sets nodes in both lengthwise and crosswise directions for the purpose of thermal calculation. There is no limitation on the number of nodes, but it is suggested to use the same meshes as what is used in neutronics calculations for convenience. No discretization of fuel meat is made in the thickness direction. Each node is independent in terms of microstructure evolution and dimensional geometric change. Neither mechanical interaction nor heat flow between neighboring nodes is considered currently. The materials property models (fuel meat thermal conductivity) and constituent volume evolution models are unaltered from what was described previously in Ref. [8][9]. Only the models which were modified or updated in current version are explained in this paper, which include thermal calculation model, Al cladding oxidation model, IL growth model, and fuel swelling model.

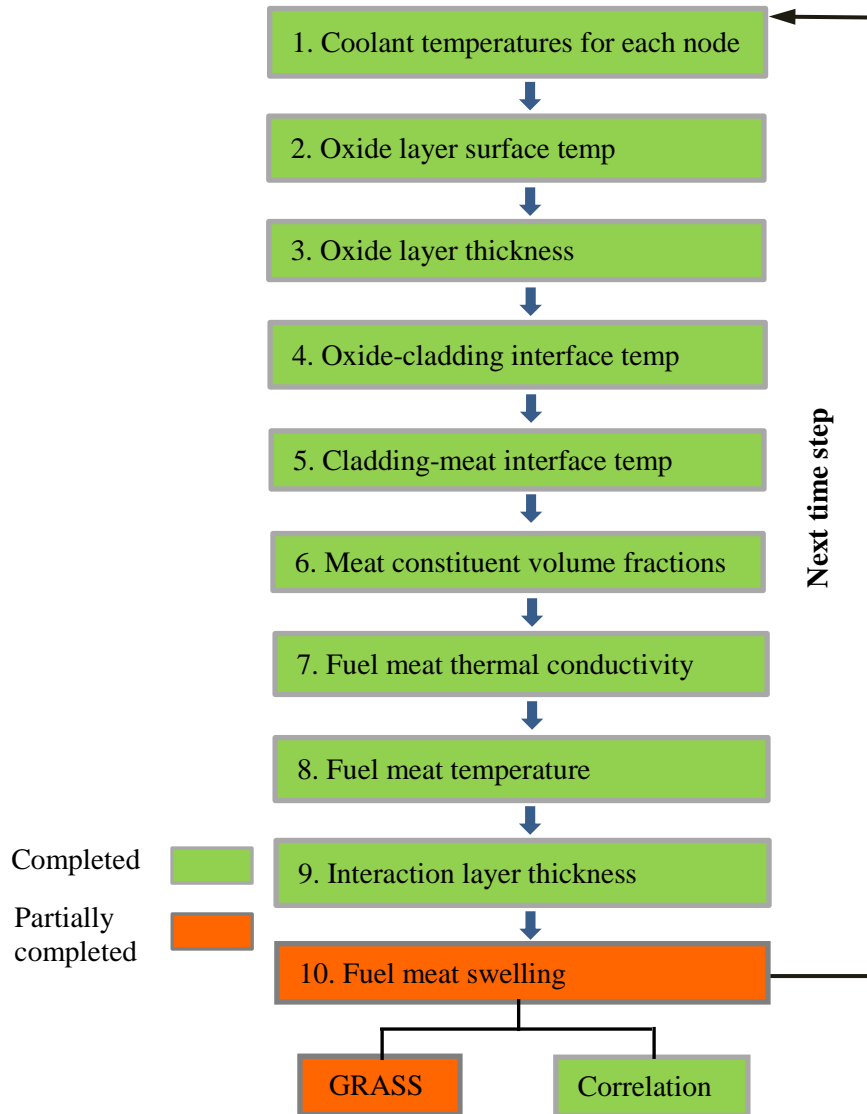


Fig. 1 Flow chart of the DART-2D framework. Different color indicates the current completion status of each function.

### Thermal calculation models

The axial node calculations start with the node nearest the coolant inlet and continue along the coolant flow direction. Coolant flow conditions, such as inlet temperature, velocity and pH value are provided as input parameters. The fuel plate heat transfer is assumed to be one-dimensional (1-D) in the plate thickness direction. The validity of the assumption lies in the fact that the thermal gradient in the thickness direction is much greater than those in the other two directions, because the smallest dimension of a full-size fuel plate is the thickness (typical dimensions of a full-size plate in EFUTURE and SELENIUM tests are ~ 1.22 mm in thickness, 5.7 cm in width, and 97 cm in length). Therefore, the heat conduction equation is simplified to be 1-D.

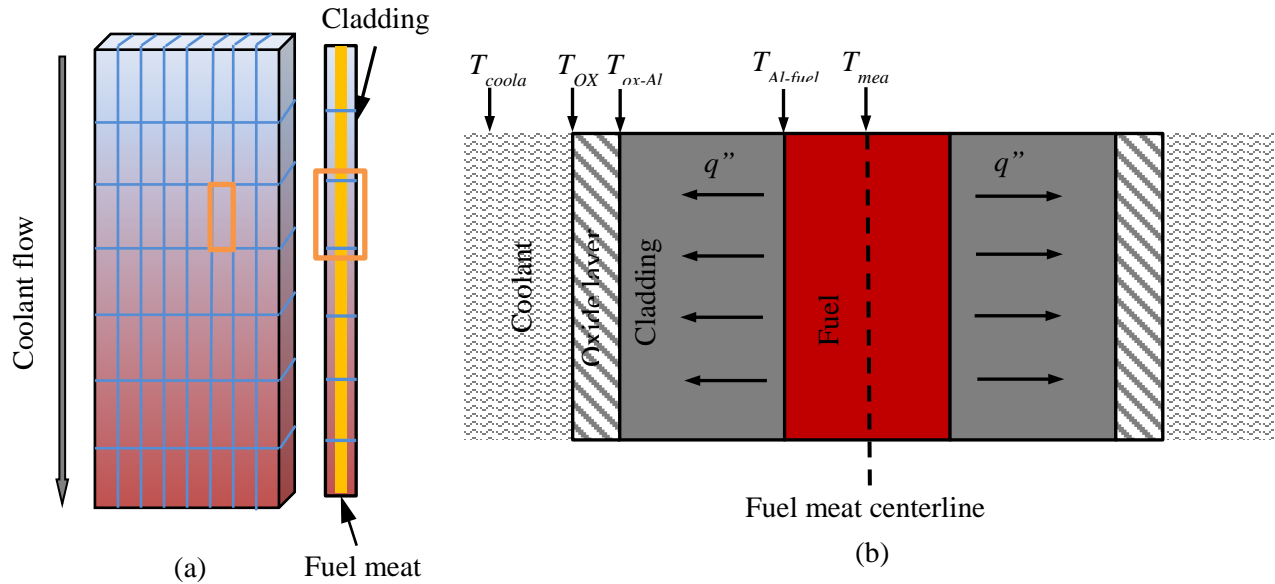


Fig.2 (a) An example of the meshing scheme in the DART-2D framework, and (b) enlarged side view of one fuel plate node indicated in (a) and schematic representation of the temperatures calculated to obtain fuel meat centerline temperatures.

Coolant temperature distribution is computed first by assuming that all heat released from the fuel plate is transferred into bulk coolant by conduction. The heat transfer coefficient between the bulk of the coolant and the oxidation layer surface is determined using the Dittus-Boelter correlation. Next, for each node, the cladding and fuel temperature calculations start from coolant ( $T_{coolant}$ ), then move layer by layer through coolant/oxidation layer interface ( $T_{ox}$ ), oxide layer/cladding interface ( $T_{ox-Al}$ ), cladding/fuel meat interface ( $T_{Al-fuel}$ ), and finally reach fuel meat centerline position ( $T_{meat}$ ), as depicted in Fig. 2(b).

$$T_{inner} = T_{outer} + \frac{q''(z) \cdot z}{k} \quad (1)$$

where:

$T_{inner}$  : inner surface temperature of the interested layer in K

$T_{outer}$  : outer surface temperature of the interested layer in K

$z$  : the layer thickness in cm

$q''(z)$ : heat flux across plate thickness in W/cm<sup>2</sup>

$k$ : thermal conductivity of the interested layer in W/(cm·K)

The terms of “inner surface” and “outer surface” above are defined according to the relative distance of the surface from the fuel meat centerline (“inner surface” is closer to the fuel meat centerline).

### Al cladding oxidation model

A layer of oxidation product forming on the water side of Al cladding increases fuel temperature because of its low thermal conductivity. In order to calculate the oxide layer thickness, multiple oxide thickness prediction models were implemented in DART-2D, including the Griess model, the Kritz model, and ANS correlation II [11], as well as an empirical model proposed by Kim et al. [11][12]. The former three models were developed based on out-of-pile data, and the last one was built using both out-of-pile and in-pile test data and recently revised to expand its applicability to high power conditions found in reactors like BR2 [12]. All calculations performed in this work used the model developed by Kim et al., in which the oxide layer thickness and the oxide surface temperature are coupled. Therefore, the oxide surface temperature obtained in the previous time step is used for the oxide layer thickness calculation in the current time step.

### Interdiffusion layer growth model

The basic IL growth correlation during irradiation for U-Mo particles in a pure Al matrix was developed by fitting the IL thicknesses measured from RERTR-4, -5, -6, -7, -9, and KOMO-4 tests [13], which is expressed as:

$$Y_0^2 = 2.6 \times 10^{-8} f^{0.5} \exp\left(-\frac{3850}{T}\right)t \quad (2)$$

where  $Y_0$  is the IL thickness in  $\mu\text{m}$ ,  $f$  fission rate in  $\text{f/cm}^3/\text{s}$ ,  $T$  fuel meat temperature in K, and  $t$  irradiation time in s. On top of the basic IL growth correlation, an IL reduction factor ( $f_{Si}$ ) as a function of fuel meat temperature ( $T$ ) and Si content ( $W_{Si}$ ) was also proposed in Ref. [13] to describe the IL reduction effect by Si addition in the Al matrix. As such, the IL growth correlation for U-Mo dispersion fuels with Si addition in the Al matrix can be expressed as:

$$Y^2 = Y_0^2 f_{Si} \quad (3)$$

where  $Y$  is the IL thickness in  $\mu\text{m}$ . The expression of  $f_{Si}$  in Ref. [13] was suggested based on the limited experimental data (RERTR-6 and KOMO-4 tests) available at that time. In order to simulate the IL growth behavior for coated particle, a revised IL reduction factor  $f_{reduction}$  is postulated here to replace  $f_{Si}$  in Eqn. (3), and it takes the form of:

$$f_{reduction} = 0.000015T, \text{ if } f \leq 8 \times 10^{14} \text{ f/cm}^3/\text{s} \quad (4)$$

and 
$$f_{reduction} = 0.0001T, \text{ if } f \geq 8 \times 10^{14} \text{ f/cm}^3/\text{s} \quad (5)$$

where  $T$  is the fuel meat centerline temperature in K. The piece-wise function in Eqns. (4) and (5) is a linear function of temperature, changing the slope at a threshold fission rate. The threshold fission rate of  $8 \times 10^{14} \text{ f/cm}^3/\text{s}$  was determined based on the observation that IL volume

fraction increased rapidly in the regions where the fission density (FD) is higher than  $4 - 4.5 \times 10^{21}$  fissions/cm<sup>3</sup>-UMo in irradiated SELENIUM plates [5]. The slopes in Eqns. (4) and (5) were obtained by fitting to the measured data from the SELENIUM plates. The fitted results will be discussed later in Section 3. Note that although  $f_{reduction}$  is expressed as a function of  $T$  in Eqns. (4) and (5), it is physically related to the fraction of damaged coating. Considering the range of temperature calculated, the typical value of  $f_{reduction}$  is ~5% in the regions where  $f \geq 8 \times 10^{14}$  f/cm<sup>3</sup>/s. The value of ~5% is consistent with the estimated damaged fraction of coating [5]. In the lower fission rate regions, fuel meat temperature is considerably lower, and IL growth is hence further inhibited. According to Eqn. (5),  $f_{reduction}$  is less than 1% in these regions, even though the damaged fraction of coating is the same. The reason for the large difference between the slopes in Eqns. (4) and (5) is that the temperature dependence in Eqn. (2) may not be valid in the low fission rate regions and needs re-evaluation.

### Fuel swelling model

Instead of using only the mechanistic model in the original DART code [8][9], DART-2D offers the options of using either the theory-based model [14] or an empirical correlation [15] for fission gas swelling calculation. The implementation of both options provides users the flexibility to select the appropriate approach to meet their specific analysis requirements. The mechanistic theory-based model permits the exploration of underlying behavioral mechanisms of fission gas swelling by providing detailed fission-gas-behavior information, such as fission gas bubble size distribution at various locations (inside grains, on grain boundaries, and at triple points) [6]. When the key parameters, for example gas atom diffusivity in U-Mo, are given, the code is able to predict fuel irradiation behavior beyond its calibration data range. The theory-based gas behavior model is composed of a series of coupled partial differential equations [6]. Consequently, it is extremely computation-costly and inefficient when running the simulation with the theoretical approach. On the other hand, the calculations with the empirical correlation [15] are inexpensive and more suitable for testing assumptions and developing correlations within a limited range of operating conditions. The calculation results presented in this paper were obtained using the empirical approach, and they will be re-assessed when the integration of the rate-theory-based gas behavior model is completed.

### **3. Simulation results and discussion**

This section presents the DART-2D simulation results of 5 selected full-size U-7Mo/Al dispersion fuel plates irradiated in the BR2 reactor. The 5 fuel plates were irradiated in 3 irradiation tests. Plates U7MC4202 and U7MC6301 were irradiated in the E-FUTURE test, which was designed to select a Si concentration added to the Al matrix and fuel plate heat treatment parameters [16]. Two plates produced with coated particles (U7MD1221-Si coated and U7MD1231-ZrN coated) were irradiated in the SELENIUM test, whose irradiation conditions were select to be close to E-FUTURE to allow direct comparisons between the two tests [18]. In order to investigate the possible fission rate effect on fuel swelling, one plate which is identical to U7MD1221 was irradiated in the SELENIUM-1a test at a lower fission rate but reached the same FD as that in SELENIUM. The fabrication characteristics and irradiation conditions of these 5 plates are summarized in Table 1.

Table 1. Fabrication characteristics and irradiation conditions of the 5 selected plates irradiated at BR2.

Test	E-FUTURE [19]		SELENIUM [19]		SELENIUM - 1a [20]
Irradiation period	2010-2011		2012		2015-2016
Plate ID	U7MC4202	U7MC6301	U7MD1221	U7MD1231	
U-Mo powder type	Atomized	Atomized	Atomized + 600nm Si	Atomized + 1 $\mu$ m ZrN	Atomized + 600nm Si
Mo content (wt%)	7.5	7.3	7.2	7.2	7.2
Enrichment (% <sup>235</sup> U)	19.8	19.8	19.8	19.8	19.8
Fuel loading (gU/cm <sup>3</sup> )	8.1	8.0	8.0	8.0	8.0
Matrix type	Al+4.1wt% Si	Al+6.0wt% Si	Al	Al	Al
Cladding material	AG3NE	AlFeNi	AG3NE	AG3NE	AG3NE
Max. heat flux BOL (W/cm <sup>2</sup> )	453	472	421	466	278
Total EFPD (days)	77	77	70	70	98
Plate average burnup (% <sup>235</sup> U)	48.1	47.5	47.9	47.5	53.1
Plate average FD (f/cm <sup>3</sup> UMo)	3.6 $\times$ 10 <sup>21</sup>	3.6 $\times$ 10 <sup>21</sup>	3.5 $\times$ 10 <sup>21</sup>	3.5 $\times$ 10 <sup>21</sup>	4.0 $\times$ 10 <sup>21</sup>
Plate max burnup (% <sup>235</sup> U)	71.3	71.4	69.2	69.6	73.5
Plate max FD (f/cm <sup>3</sup> UMo)	5.5 $\times$ 10 <sup>21</sup>	5.5 $\times$ 10 <sup>21</sup>	5.3 $\times$ 10 <sup>21</sup>	5.3 $\times$ 10 <sup>21</sup>	5.5 $\times$ 10 <sup>21</sup>
Life average fission rate (f/cm <sup>3</sup> UMo/s)	5.4 $\times$ 10 <sup>14</sup>	5.4 $\times$ 10 <sup>14</sup>	5.8 $\times$ 10 <sup>14</sup>	5.4 $\times$ 10 <sup>14</sup>	4.7 $\times$ 10 <sup>14</sup>

The simulations were performed using fabrication characteristics, nominal plate dimensions, and coolant conditions provided by SCK-CEN. Also provided were power profiles for various times during the irradiation. The duration of each time step was 1 day in the calculations. The number of nodes is 12 in the horizontal direction and 18 in the axial direction for fuel meat in all calculations, which was set up to be the same as what was defined in neutronics calculations. Six size groups were used to represent the fuel particle size distribution profile in this study, which has a great impact on calculated IL volume fraction. An average particle size of ~70 $\mu$ m and ~50  $\mu$ m was applied for the SELENIUM/SELENIUM-1a plates and for the E-FUTURE plates, respectively. The former value is a standard size for fuel powder manufactured at KAERI (Korean Atomic Energy Research Institute), and the later one was estimated based on cross-section SEM micrographs of E-FUTURE plates in Ref.[18].

Comparisons were made between DART-2D calculation results and experimental data for fuel meat swelling and constituent volume fractions at the end of irradiation. Measured fuel meat

swelling was converted from measured plate swelling [3][17], assuming no swelling of the Al. Fuel meat constituent volume fractions were measured from the SEM micrographs of fuel plate cross sections. In order to reveal the fuel microstructure evolution as a function of burnup, several samples were sliced out at different locations of each fuel plate [18]. All measurement data employed for comparison in this study were obtained at the end of irradiation and then plotted against the FD at the corresponding location. The calculated curves shown below were generated in a similar fashion, using the calculation results of each node at the end-of-cycle (EOC), to ensure the validity of the comparisons.

*SELENIUM test*

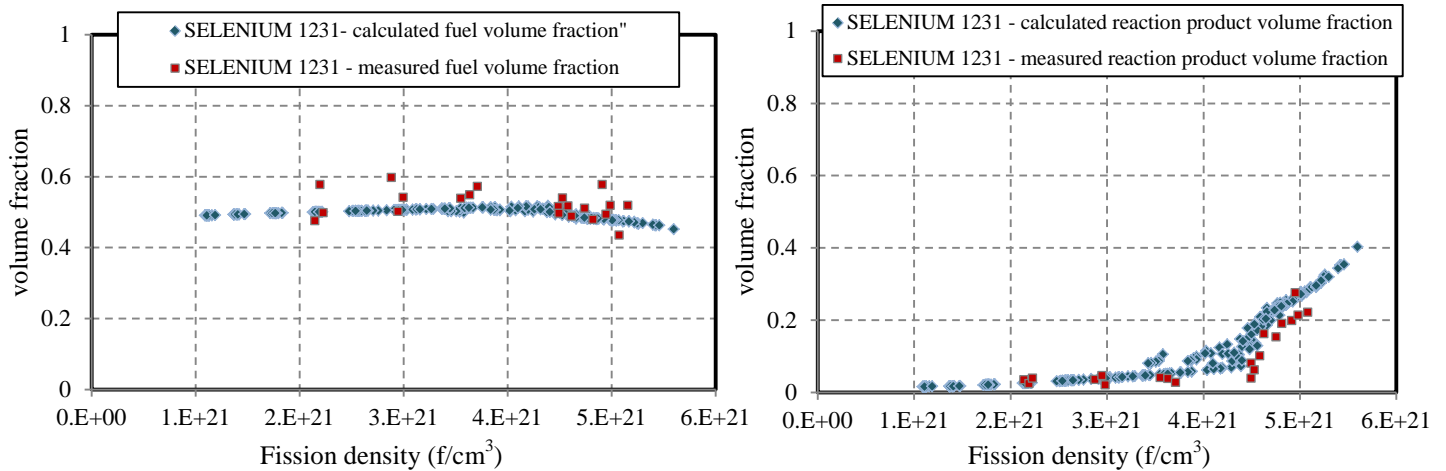


Fig. 3 Calculated fuel and IL volume fractions in the SELENIUM U7MD1231 plate, compared to experimental data [21].

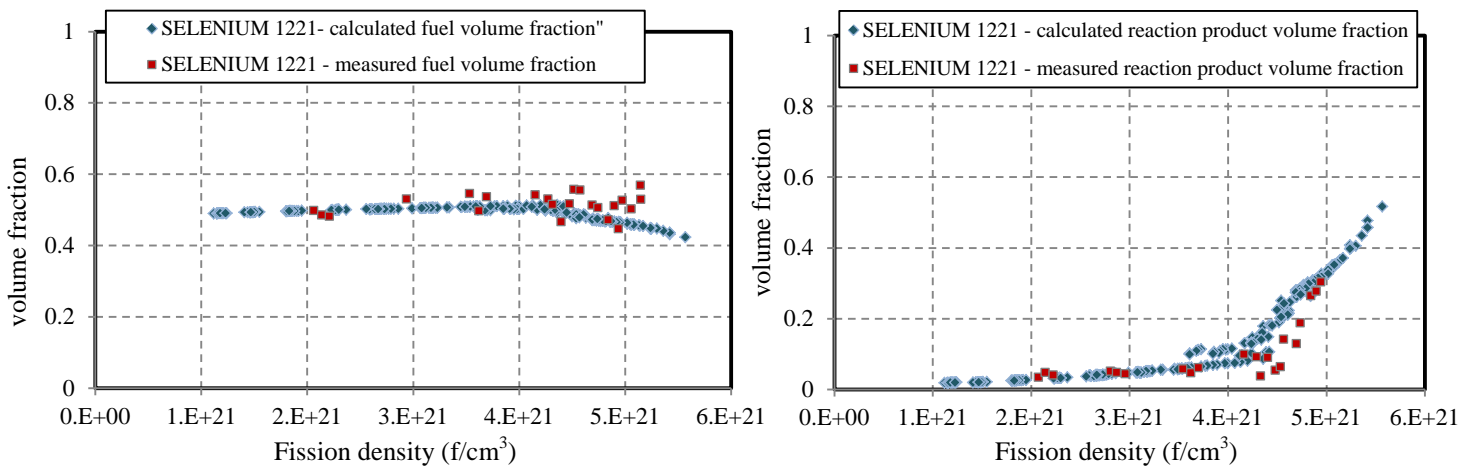


Fig. 4 Calculated fuel and IL volume fractions in the SELENIUM U7MD1221 plate, compared to experimental data [21].

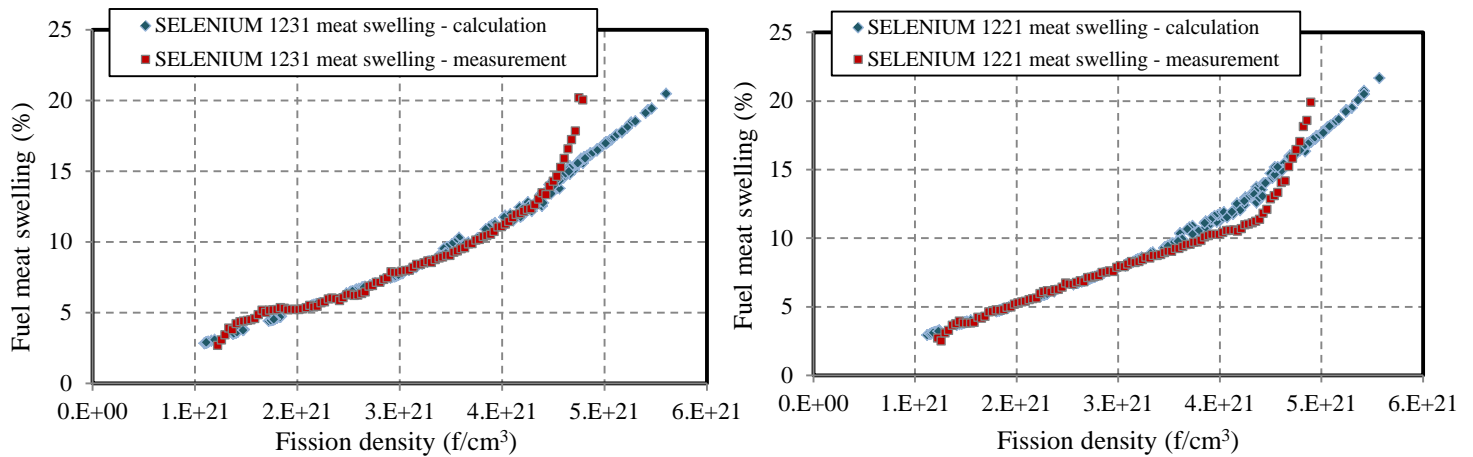


Fig. 5 Comparisons of calculated and measured fuel meat swelling [4] of the SELENIUM U7MD1231 and U7MD1221 plates.

The coefficients of linear correlations in Eqns. (4) and (5) were best fitted to the measured fuel meat swelling and constituent volume fractions of SELENIUM plates. Reasonable agreement was obtained in all comparisons shown in Figs. 3-5, which indicates certain level of confidence that Eqns. (4) and (5) can plausibly describe the IL reduction effect of coated particles.

It is noticed that in Fig. 5, the computational results generally agree with the measured fuel meat swelling over a FD range up to  $\sim 4.5 \times 10^{21}$  f/cm<sup>3</sup>-UMo, but the two curves deviate at higher FD in both plates. One possible reason that may contribute to the discrepancy at high FD is that void formation/tearing of the matrix was seen in high FD regions [4] but is not modeled in DART-2D yet.

SELENIUM-1a test

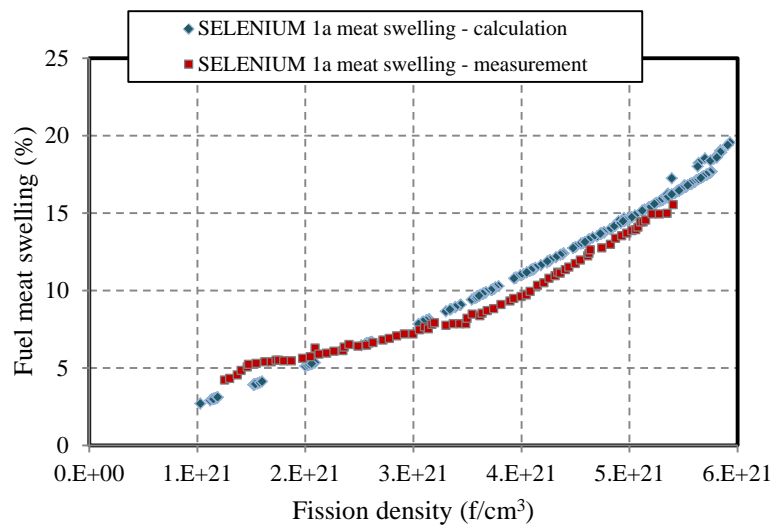


Fig. 6 A comparison of calculated and measured fuel meat swelling of the SELENIUM-1a plate.

The SELENIUM-1a plate, identical to the SELENIUM U7MD1221 plate, was irradiated in the BR2 reactor at lower power than the SELENIUM test. The same  $f_{reduction}$  fitted to the SELENIUM plates was also applied to the simulation of SELENIUM-1a test. The comparison

shown in Fig. 6 demonstrates that the postulated  $f_{reduction}$  reasonably reproduce the fuel meat swelling behavior of this plate. The good agreement in Fig. 6 implies that some microstructural changes in fuel meat, related to the acceleration of fuel meat swelling at high FD, may not develop fully during this test, for example the void formation/tearing of fuel meat at particle/matrix interfaces. This prediction will be verified when the destructive analyses are performed. The constituent volume fractions of fuel meat are to be measured as a part of the destructive analyses, and will be compared with calculation results when the data becomes available.

E-FUTURE test

Two major differences in fabrication parameters exist between E-FUTURE and SELENIUM/SELENIUM-1a plates: average fuel particle size (~50 μm for E-FUTURE vs. ~70 μm for SELENIUM) and IL reduction method (Si addition in the matrix in E-FUTURE vs. coated particle in SELENIUM). The fuel particle size distribution inputted for the simulation of E-FUTURE plates was estimated based on its post irradiation SEM micrographs in Ref. [18]. The IL reduction factor used for the simulation of E-FUTURE plates is:

$$f_{reduction} = 0.0001T \tag{6}$$

It has the same formulation as Eqn. (5) but was applied to the entire fission rate range. No threshold fission rate was selected to distinguish IL growth behavior in different fission rate/temperature regimes. This is because the measured IL volume fraction data points are too scarce to show any transition tendency at high FD. Eqn. (6) is proposed here to test whether the linear temperature correlation is able to capture the main characteristics of irradiation behavior of the fuel plates with Si addition in the matrix. Further validation of Eqn. (6) will be performed by simulating additional tests with Si addition in the matrix. The simulation results of two E-FUTURE plates using Eqn. (6) are presented in the figures below.

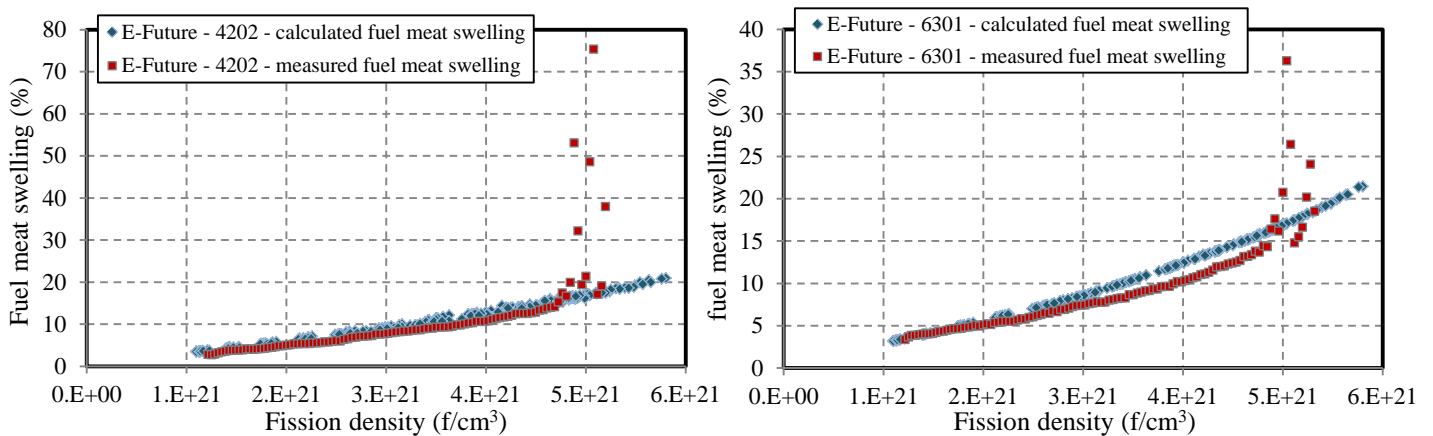


Fig. 7 A comparison of calculated and measured fuel meat swelling of the E-FUTURE U7MC4202 and U7MC6301 plates [17].

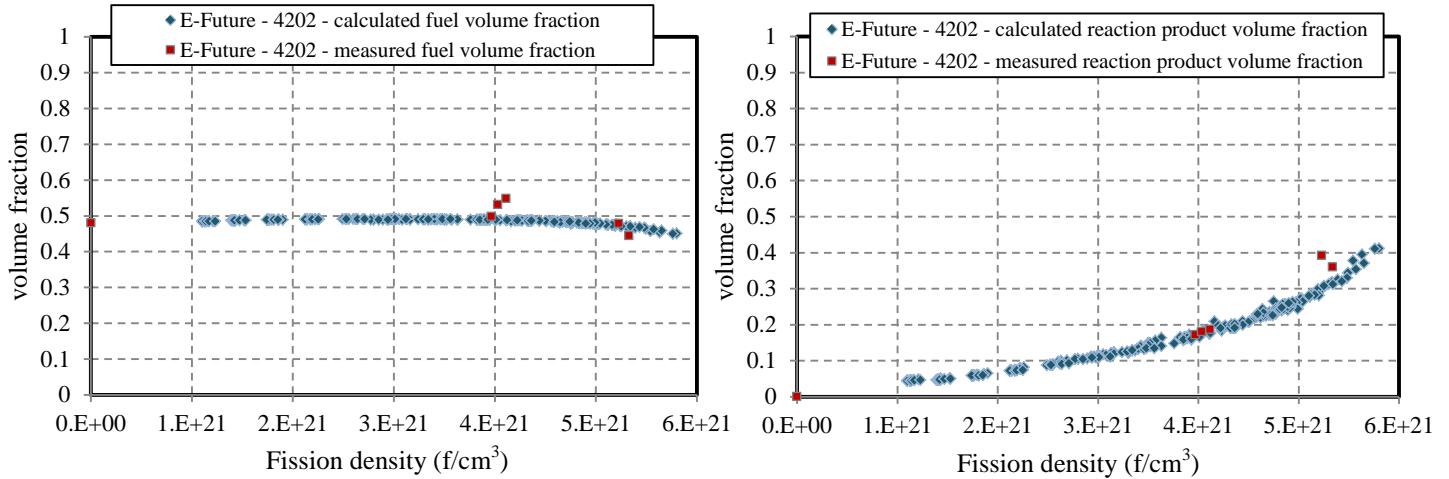


Fig. 8 Calculated fuel and IL volume fractions in the E-FUTURE U7MC4202 plate, compared to experimental data [22].

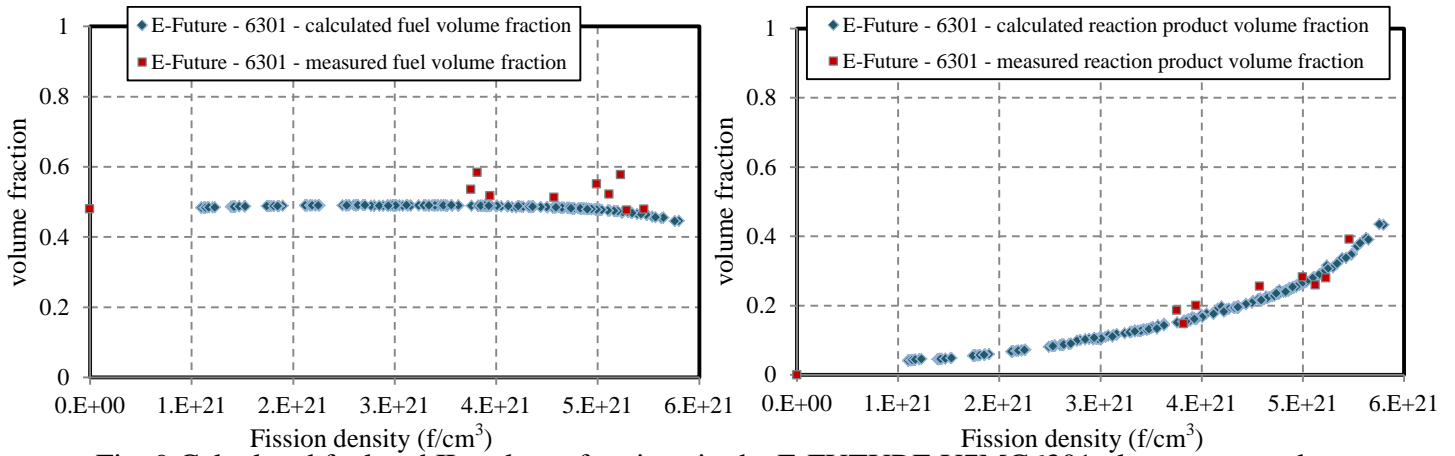


Fig. 9 Calculated fuel and IL volume fractions in the E-FUTURE U7MC6301 plate, compared to experimental data [22].

The comparisons in Figs. 7-9 show a good agreement between the calculation and measurement. In the pillowed regions ( $FD > 4.8 \times 10^{21}$  f/cm<sup>3</sup> UMo), large fission-gas-filled pores formed at the interfaces of fuel particles and the matrix in these regions, and this is the main origin of the discrepancies between calculated and measured fuel meat swelling at high FD regions ( $FD > 4.8 \times 10^{21}$  f/cm<sup>3</sup> UMo) in Fig. 7. Figs. 8 and 9 present the calculated and measured fuel and IL volume fractions at EOC of the E-FUTURE U7MC4202 and U7MC6301 plates respectively. The comparison results in Figs. 8 and 9 demonstrate that using the IL reduction factor in Eqn. (6) was adequate to reasonably capture the composition evolution in the E-FUTURE plates.

## Representative fuel meat temperature profiles

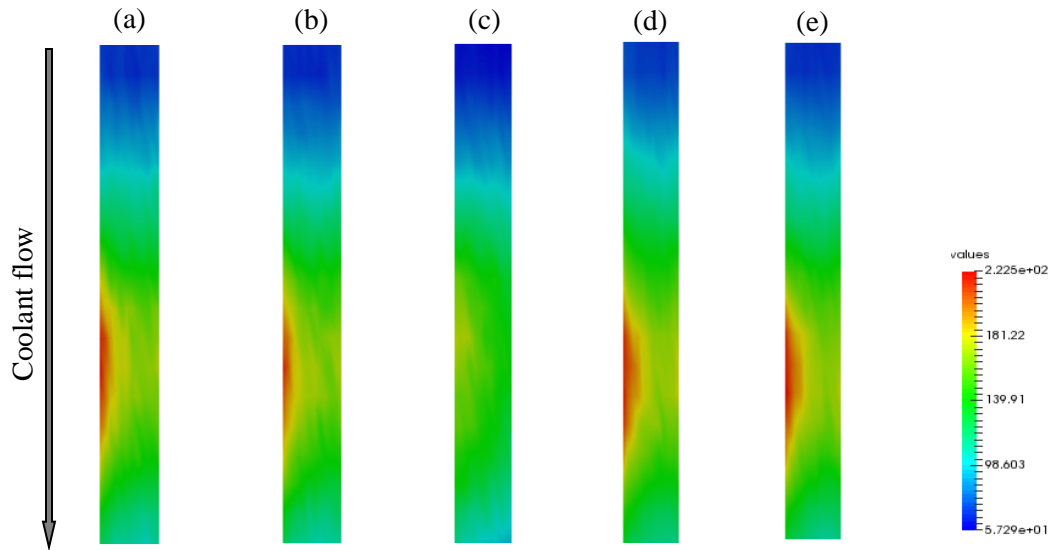


Fig. 10 Representative fuel meat centerline temperature distributions in (a) the SELENIUM 1221 plate, (b) the SELENIUM 1231 plate, (c) the SELENIUM-1a plate, (d) the E-FUTURE 4202 plate, and (e) the E-FUTURE 6301 plate.

The generally good agreement between experimental and calculated fuel meat swelling and constituent volume fractions of all 5 plates supports the plausibility of fuel meat temperatures calculated with DART-2D. Fuel meat centerline temperature profiles were estimated at each time step. Fig. 10 shows the most representative temperature profile during the irradiation of each plate. Given the materials properties and models used, the temperatures of these plates are in a range of 60- 220°C. The temperature distributions in Fig. 10 also indicate that the SELENIUM-1a plate has lower temperatures than other plates because of its lower power. The hottest spots in all plates in Fig. 10 are consistent with the location where the plates swell most [3][17].

## 4. Conclusion

The dispersion fuel performance code DART are being restructured to improve its capability in simulating full-size dispersion fuel plates and to enhance its flexibility to meet different application requirements. In this study, a 2-D FORTRAN framework for the DART code was developed to enable time-dependent fuel temperature estimations throughout a fuel plate in both longitudinal and lateral directions, using provided power histories and fuel plate fabrication parameters as inputs. Accordingly, important temperature-sensitive irradiation responses of fuel plate, such as oxide layer growth, fuel meat thermal conductivity degradation, IL growth, and fuel meat constituent volume fractions, are updated for each node at each time step. At the end of irradiation, the calculated fuel meat swelling profile and constituent volume fractions can be obtained and compared to measurement data.

Fuel meat swelling and constituent volume fractions in 5 selected full-size U-7Mo/Al dispersion fuel plates irradiated in the BR2 reactor were estimated using the 2-D framework. The calculated results are in reasonably good accordance with the measurement. In order to simulate the irradiation behavior of fuel plates with coated particle or with Si addition in the

matrix, a piece-wise IL reduction factor was proposed and applied in the simulation. Fuel meat centerline temperatures of all plates were estimated and provided for the potential analyses of the temperature effect on IL growth. The simulation exercises in this work not only provide the hard-to-measure parameters of fuel plates during irradiation, but also exhibit that the code is an effective tool in developing correlations and in identifying the key variables in dispersion fuel performance under irradiation.

## 5. Acknowledgement

This work was supported by the U.S. Department of Energy, Office of Materials Management and Minimization (NA-23), National Nuclear Security Administration, under Contract No. DE-AC-02-06CH11357 between UChicago Argonne, LLC and the Department of Energy.

## 6. References

- [1] G.L. Hofman, Y.S. Kim, M.R. Finlay, J.L. Snelgrove, S.L. Hayes, M.K. Meyer, C.R. Clark, F. Huet, "Post-irradiation analysis of low enriched U-Mo/Al dispersion fuel miniplate tests, RERTR 4 & 5," in: *Proceedings of the 26<sup>th</sup> International Meeting on Reduced Enrichment for Research and Test Reactors (RERTR)*, Vienna, Austria, 2004.
- [2] A. Leenaers, S. Van den Berghe, C. Detavernier, "Surface engineering of low enriched uranium-molybdenum," *J. Nucl. Mater.*, 440, 220-228, 2013.
- [3] S. Van den Berghe, Y. Parthoens, G. Cornelis, A. Leenaers, E. Koonen, V. Kuzminov, C. Detavernier, "Swelling of U(Mo) dispersion fuel under irradiation – non-destructive analyses of the SELENIUM plates," *J. Nucl. Mater.*, 442, 60-68, 2013.
- [4] A. Leenaers, S. Van den Berghe, E. Koonen, V. Kuzminov, C. Detavernier, "Fuel swelling and interaction layer formation in the SELENIUM Si and ZrN coated U(Mo) dispersion fuel plates irradiated at high power in BR2," *J. Nucl. Mater.*, 458, 380-393, 2015.
- [5] B. Ye, G.L. Hofman, A. Leenaers, "On the efficiency of diffusion barrier coating on U-Mo fuel particles in dispersion fuels," *Proceedings of the 20<sup>th</sup> International Meeting on Research Reactor Fuel Management (RRFM)*, Berlin, Germany, March 13-17, 2016.
- [6] J. Rest, "The DART dispersion analysis research tool: a mechanistic model for predicting fission-product-induced swelling of aluminum dispersion fuels," ANL-95/36, Argonne National Laboratory (1995).
- [7] H. Taboada, R. Saliba, M. V. Moscarda, J. Rest, "Thermomechanical DART code improvements for LEU VHD dispersion and monolithic fuel element analysis," *Proceedings of the 26<sup>th</sup> International Meeting on Reduced Enrichment for Research and Test Reactors (RERTR)*, Vienna, Austria, November 7-12, 2004.
- [8] B. Ye, J. Rest, Y.S. Kim, "A description of the mechanistic DART-THERMAL dispersion fuel performance code and application to irradiation behavior analysis of U-Mo/Al," ANL/GTRI/TM-13/3, Argonne National Laboratory (2013).
- [9] B. Ye, J. Rest, Y.S. Kim, G. Hofman, B. Dionne, "DART analysis of irradiation behavior of U-Mo/Al dispersion fuels," *Nucl. Technol.*, 191, 27-40, 2014.
- [10] D.M. Wachs, A.B. Robinson, F.J. Rice, N.C. Kraft, S.C. Taylor, M. Lillo, N. Woolstenhulme, G.A. Roth, "Swelling of U-7Mo/Al-Si dispersion fuel plates under irradiation – non-destructive analysis of the AFIP-1 fuel plates," *J. Nucl. Mater.*, 476, 270-292, 2016.

- [11] Y.S. Kim, G.L. Hofman, A.B. Robinson, J.L. Snelgrove, N. Hanan, "Oxidation of aluminum alloy cladding for research and test reactor fuel," *J. Nucl. Mater.*, 378, 220-228, 2008.
- [12] Y.S. Kim, "Revised Al cladding oxidation model," Intra-laboratory memo, Argonne National Laboratory, 2016.
- [13] Y.S. Kim, G.L. Hofman, H.J. Ryu, J.M. Park, A.B. Robinson, D.M. Wachs, "Modeling of interaction layer growth between U-Mo particles and an Al Matrix," *Nucl. Eng. Technol.*, 45, 827-838, 2013.
- [14] J. Rest, "GRASS-SST: a comprehensive, mechanistic model for the prediction of fission-gas behavior in UO<sub>2</sub>-base fuels during steady-state and transient conditions," NUREG/GR-2437 Vol. I, ANL-78-53, Argonne National Laboratory (1978).
- [15] Y.S. Kim, G.L. Hofman, "Fission product induced swelling of U-Mo alloy fuel," *J. Nucl. Mater.*, 419, 291-301 (2011).
- [16] X. Iltis, F. Charollais, M. C. Anselmet, P. Lemoine, A. Leenaers, S. Van den Berghe, E. Koonen, C. Jarousse, D. GESlin, F. Frery, H. Guyon, in: *Proceedings of the 32<sup>nd</sup> International Meeting on Reduced Enrichment for Research and Test Reactors (RERTR)*, Lisbon, Portugal, 2010.
- [17] S. Van den Berghe, Y. Parthoens, F. Charollais, Y.S. Kim, A. Leenaers, E. Koonen, V. Kuzminov, P. Lemoine, C. Jarousse, H. Guyon, D. Wachs, D. Keiser Jr, A. Robinson, J. Stevens, G. Hofman, "Swelling of U(Mo)-Al(Si) dispersion fuel under irradiation – non-destructive analyses of the LEONIDAS E-FUTURE," *J. Nucl. Mater.*, 430, 246-258 (2011).
- [18] A. Leenaers, "Surface-engineered low-enriched Uranium-Molybdenum fuel for research reactors," PhD thesis 2014, University of Ghent-SCK·CEN, ISBN-9789076971223.
- [19] S. Van den Berghe, P. Lemoine, "Review of 15 years of high-density low-enriched UMo dispersion fuel development for research reactors in Europe," *Nucl. Eng. Technol.*, 125-146 (2014).
- [20] V. Kuzminov, "Evaluation of irradiation conditions for U-Mo LEU 'SELENIUM-1A' fuel plate during BR2 cycles 02/2014 – 01/2015," SCK·CEN-R-0000, SCK·CEN (2015).
- [21] A. Leenaers, S. Van den Berghe, presented at *the 18th International Meeting on Research Reactor Fuel Management (RRFM)*, Ljubljana, Slovenia, Mar. 30-Apr. 3 (2014).
- [22] A. Leenaers, J. Van Eyken, S. Van den Berghe, E. Koonen, F. Charollais, P. Lemoine, Y. Calzavara, H. Guyon, C. Jarousse, B. Stepnik, D. Wachs, A. Robinson, in: *Proceedings of the 16th International Meeting on Research Reactor Fuel Management (RRFM)*, Prague, Czech Republic, March 18-22 (2012).